Journal of
Nanoscience and Nanotechnology
Vol. 12, 1–8, 2012

Comparative *In Vitro* Cytotoxicity Study on Uncoated Magnetic Nanoparticles: Effects on Cell Viability, Cell Morphology, and Cellular Uptake

L. Li[1], K. Y. Mak[1], J. Shi[2], H. K. Koon[2], C. H. Leung[1], C. M. Wong[3, 4], C. W. Leung[5], C. S. K. Mak[6], N. M. M. Chan[7], W. Zhong[8], K. W. Lin[9], E. X. Wu[1], and P. W. T. Pong[1, *]

[1] *Department of Electrical and Electronic Engineering, The University of Hong Kong, Hong Kong*
[2] *Department of Physics, Hong Kong Baptist University, Hong Kong*
[3] *Department of Pathology, The University of Hong Kong, Hong Kong*
[4] *State Key Laboratory for Liver Research, The University of Hong Kong, Hong Kong*
[5] *Department of Applied Physics, Hong Kong Polytechnic University, Hong Kong*
[6] *Department of Chemistry, The University of Hong Kong, Hong Kong*
[7] *Department of Surgery, University of Cambridge, United Kingdom*
[8] *Department of Physics, Nanjing University, China*
[9] *Department of Materials Science and Engineering, National Chung Hsing University, Taiwan*

Magnetic iron oxide nanoparticles (MIONPs) must be biocompatible, and a thorough knowledge on their potential cytotoxicity is crucial for their biomedical applications. However, the detailed study about the effects of iron oxide nanoparticles on cell viability, cell morphology, and cellular uptake of different mammalian cells is still insufficient. In this paper, comparative cytotoxicity study of uncoated magnetite nanoparticles at different concentrations was performed on human cervical cancer cell line (HeLa) and immortalized normal human retinal pigment epithelial cell line (RPE). The size, structure, and magnetic behavior of the MIONPs were characterized using transmission electron microscopy (TEM), X-ray diffractometry (XRD), and vibrating sample magnetometry (VSM) respectively. After 24-hour incubation with the MIONPs, the cell viability was determined by live/dead assay, the cell morphology at high magnification was observed under scanning electron microscopy (SEM), and the cellular uptake of MIONPs was measured under TEM and verified by energy-dispersive X-ray spectroscopy (EDX) analysis. Our results indicate that the uncoated MIONPs at a high concentration (0.40 mg/ml) were toxic to both HeLa and RPE cells. However, the cytotoxicity of uncoated MIONPs at low concentrations was cell-type specific, and RPE cells were more susceptible to these MIONPs than HeLa cells. The effects of the MIONPs on cell morphology and the nanoparticles uptake also showed different features between these two cell lines. Hence cell type should be taken into consideration in the *in vitro* cytotoxicity study of uncoated MIONPs. Additionally, it should be noticed that the cell morphological changes and the uptake of nanoparticles can take place even though no toxic effect of these MIONPs at low concentrations was reflected in the traditional cell viability assay.

Keywords: Magnetic Nanoparticle, HeLa Cell, RPE Cell, Cytotoxicity, Cell Morphology.

RESEARCH ARTICLE

1. INTRODUCTION

Magnetic iron oxide nanoparticles (MIONPs) have attracted increasing interests in many biomedical areas, such as magnetic resonance imaging (MRI) contrast enhancement,[1–3] cell labeling,[4, 5] magnetofection,[6] drug delivery,[7, 8] and magnetic hyperthermia.[9, 10] Magnetic nanoparticles are considered to be biocompatible until recent studies calling it into question. Various degrees of cell death induced by magnetic nanoparticles have been found in human dermal fibroblasts,[11–15] mouse fibroblast cells,[16–19] human umbilical vein endothelial cells,[20] and rat pheochromocytoma cells.[21]

Iron oxide nanoparticles are usually coated with inorganic materials and organic materials, such as silica, gold, dextran, polyethylene glycol (PEG), polyvinyl alcohol (PVA), alginate, chitosan, and other polymers.[22] The coating can improve the stability of nanoparticles in solution,

*Author to whom correspondence should be addressed.

enhance the bonding of various biological ligands to nanoparticle surfaces, and ensure the biocompatibility of nanoparticles. However, the coating of nanoparticles may be damaged during the process of applications. For example, the ZnS shell of nanoparticles can be ruptured when the oral ingestion exposes the material to the low pH environment of the stomach.[23] It was also reported that the dextran shells on nanoparticles can be broken down upon cell internalization.[24] These situations may expose the toxicity of uncoated iron oxide nanoparticles which are the common cores used in magnetic nanoparticle manufacturing. Thus the biocompatibility study on uncoated MIONPs is very important and it will facilitate further applications of MIONPs in the biomedical areas.[25–27]

However, the uptake and biocompatibility of nanoparticles are not only dependent on the particle size and surface but also related to the cell type.[28] For instance, Xia and co-workers demonstrated that NH_2-labeled polystyrene nanospheres were highly toxic in macrophage (RAW 264.7) and epithelial (BEAS-2B) cells, while human microvascular endothelial (HMEC), hepatoma (HEPA-1), and pheochromocytoma (PC-12) cells were relatively resistant to nanoparticle injury.[29] So it is necessary to study the respective cellular responses of different cell lines to the same kind of magnetic nanoparticle.

In this study, the biological responses of the two cell lines to the uncoated MIONPs were investigated. These two cell lines were the cervical cancer cell line (HeLa) and the immortalized normal human cell line (RPE, retinal pigment epithelial). The main reason for choosing these two cell lines is because both of them are often exposed to magnetic nanoparticles in many situations. For example, the tumor drug delivery by magnetic nanoparticles has raised extensive interests. Kohler et al. prepared methotrexate-modified superparamagnetic nanoparticles to target human cervical cancer cells.[30] Magnetic nanoparticles have also been introduced in eye drops as clinical therapy to treat cancers.[31] In this case, the nanoparticles should be biocompatible with normal retinal cells.[20, 32]

Since tagging may alter the characteristics and toxicity of nanoparticles,[25] the uncoated MIONPs used in this experiment were not functionalized. We characterized these MIONPs by using transmission electron microscopy (TEM), X-ray diffractometry (XRD), and vibrating sample magnetometry (VSM), examined their toxicity on cell viabilities by live/dead assay, and compared the cell morphological changes and the nanoparticle uptake induced in the RPE cells with the HeLa cells.

2. EXPERIMENTAL DETAILS

2.1. Magnetic Iron Oxide Nanoparticles

The MIONPs (Fe_3O_4, 99.5%, 25 nm, spherical) purchased from Nanostructured and Amorphous Materials (USA) were used in this work. TEM (Philip Tecnai G2 20 S-TWIN) operating at 200 kV accelerating potential was used to observe the structures and dimensions of the nanoparticles. The XRD pattern of these nanoparticles was obtained using X-ray diffractometer (Mac Science, MXP-3) over the 2 theta range of 20 to 80 degrees. The magnetic measurement of these nanoparticles was carried out by VSM (Lakeshore 7400) at room temperature.

2.2. Cell Culture and Treatment

HeLa cells were maintained in DMEM medium (Invitrogen) supplemented with 10% fetal bovine serum (FBS, Invitrogen), penicillin (50 U/ml, Invitrogen), and streptomycin (50 μl/ml, Invitrogen). RPE cells were maintained in DMEM/F12K (50:50) medium supplemented with 10% fetal bovine serum (FBS, Invitrogen), penicillin (50 U/ml, Invitrogen), and streptomycin (50 μl/ml, Invitrogen). The cells were grown and maintained in 5% CO_2 humidified incubator at 37 °C.

The MIONPs were freshly dispersed in the cell culture medium by sonication for 30 minutes and vortexed for 15 seconds at room temperature. Then they were diluted into different concentrations (0.01 mg/ml, 0.05 mg/ml, 0.20 mg/ml, and 0.40 mg/ml). In the treatment groups, HeLa cells and RPE cells were cultured in medium with the MIONPs for 24 hours. After that, live/dead assay, SEM and TEM observations were performed. Cells incubated in culture medium without the MIONPs served as the control group in each experiment.

2.3. Cell Viability Assay

Cells were seeded at a density of 5×10^3 cells/well in 96-well plates and grew overnight. The cells were then treated with various concentrations of MIONPs (0–0.40 mg/ml). After another 24 hours, the live/dead viability/cytotoxicity kit for mammalian cells (Invitrogen) was used. The cells were incubated with calcein AM (2 μM) and ethidium homodimer-1 (EthD-1, 4 μM) for 30–45 minutes at room temperature. The fluorescent images of five random fields in each well were taken by Image Xpress Micro (Molecular Devices), and a total of at least 200 cells were counted in each area using ImageJ. The total cell number was normalized to the control group treated with no MIONPs in the culture medium.

2.4. SEM of Cell Morphology

After 24-hour incubation with the MIONPs, the cells were washed by sodium cacodylate buffer, and then fixed with 2.5% glutaraldehyde buffered in sodium cacodylate for 1 hour. The samples were washed with sodium cacodylate buffer for 3 times, and dehydrated through a series of alcohol concentrations (25%, 50%, 70∼75%, 90∼95%, 100%), and subjected to critical-point drying (Bal-Tec CPD 030). The samples were then coated with gold and examined by SEM (Hitachi S-4800 FEG).

2.5. TEM Observation and EDX Analysis of Cellular Uptake

After 24-hour incubation with the MIONPs, the cells were washed by PBS, trypsinized, and then collected in 15 ml centrifuge tubes. Cells were washed by sodium cacodylate buffer, fixed with 2.5% glutaraldehyde buffered in sodium cacodylate for 4 hour, then transferred to micro-centrifuge tubes, and washed with sodium cacodylate buffer for 3 times. After that, the cells were stained in 1% osmium tetroxide for 30 minutes, washed with sodium cacodylate buffer for 3 times. Pre-warmed agar solution (60 °C) was added onto the cell pellets. The cell pellets were cut into four cubes and transferred into small glass bottles, then dehydrated through a series of alcohol concentrations (50%, 70%, 90%, and 100%), followed by propylene oxide, and finally infiltrated with 1:1 epoxy resin/propylene oxide mixture for overnight. The cell blocks were subsequently filtrated with fresh epoxy resin for 1 hour 30 minutes at 37 °C, with the help of vacuum oven, then were embedded in fresh epoxy resin in plastic capsules and polymerized at 60°C overnight. Ultrathin sections were cut using a Leica Ultracut UCT, mounted on carbon-coated copper grids and viewed without staining under TEM (Philips EM208s). The presence of iron oxide nanoparticles was verified by energy-dispersive X-ray spectroscopy (EDX) analysis.

2.6. Statistical Analysis

All the data were presented as means ± standard deviations. Statistical significance was determined by one-way analysis of variance (ANOVA).

3. RESULTS AND DISCUSSION

To evaluate the physical properties of the MIONPs, the uncoated Fe_3O_4 nanoparticles were examined under TEM. The iron oxide nanoparticles showed a spherical morphology and an average size of around 25 nm (Fig. 1). The selected area diffraction pattern (the inset in Fig. 1) shows a characteristic diffraction pattern of the magnetite nanoparticles. The XRD pattern (Fig. 2) also indicates the existence of Fe_3O_4 nanoparticles. Magnetic hysteresis curve of the MIONPs was measured at room temperature by VSM. As shown in Figure 3, the coercivity of the MIONPs is about 45 Oe at room temperature. A saturation magnetization of 46 emu/g was measured, which is lower than that of the bulk value of Fe_3O_4 (92 emu/g). Although coercivity was exhibited by the MIONPs, the small remanence of the MIONPs ($M_r \sim 0.09 M_s$) means that they do not agglomerate in absence of an external field, in a way similar to superparamagnetic nanoparticles.

To study the cytotoxicity of the MIONPs on mammalian cells, standard evaluation of acute toxicity to the cells was performed by using live/dead assay. Calcein AM can easily enter cells by diffusion and it is converted to calcein

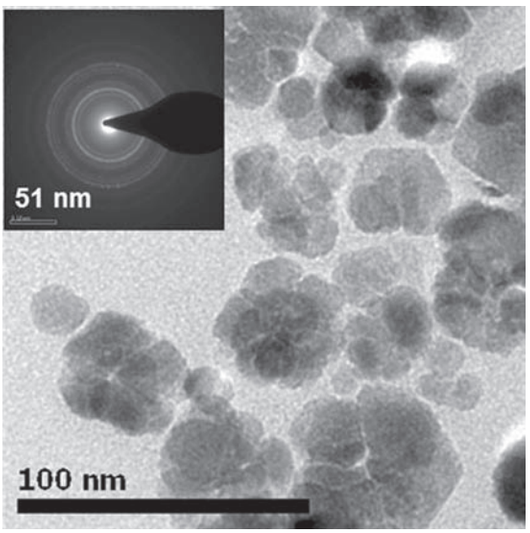

Fig. 1. TEM bright-field image of the MIONPs. The inset shows a characteristic diffraction pattern of the magnetite nanoparticles.

by the intracellular esterase which stains the live cells green. The damaged or dead cells are stained red with EthD-1. The fluorescent images of the HeLa cells and the RPE cells after 24-hour exposure to the MIONPs are shown in Figure 4. The total cell numbers of the HeLa cells and the RPE cells were counted and normalized to the corresponding control groups (Fig. 5). The exposure to the MIONPs resulted in a dose-dependent cytotoxicity on the RPE cells after the initial 24-hour exposure to the MIONPs. At the concentration range from 0.01 mg/ml to 0.40 mg/ml of the MIONPs, the total numbers of the RPE cells significantly decreased to around 86%, 75%, 64%, and 57% of their control groups. On the other hand, the MIONPs with lower concentrations did not show acute cytotoxicity on the HeLa cells, which was also observed by other researchers.[27, 33] Only when the concentration of MIONPs increased to 0.40 mg/ml, the cell number of the HeLa cells

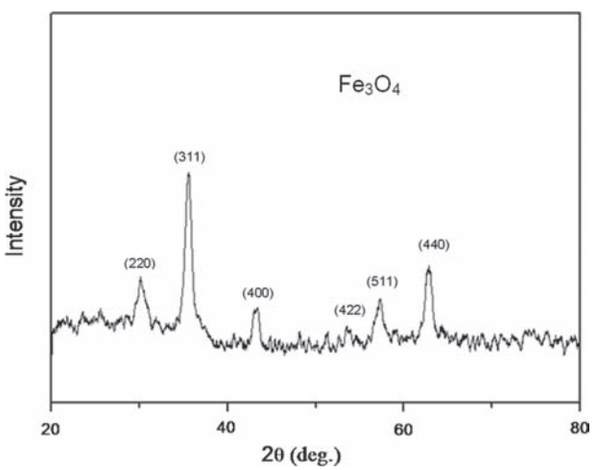

Fig. 2. XRD pattern of the MIONPs.

RESEARCH ARTICLE

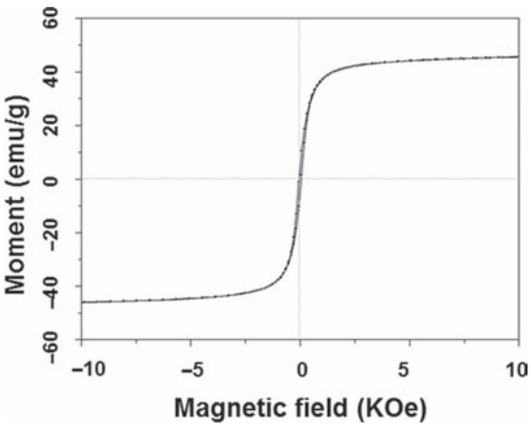

Fig. 3. Magnetic hysteresis curve of the MIONPs measured by VSM at room temperature. The saturation magnetization is 46 emu/g and the coercivity is 45 Oe.

reduced significantly. This indicates that the MIONPs at high concentration (0.40 mg/ml) were toxic to both the RPE cells and HeLa cells, while the cytotoxicity of MIONPs at low concentrations exhibited specificity to cell-type.

To study the cell morphological change in response to the MIONPs, SEM images of the HeLa cells (Fig. 6) and the RPE cells (Fig. 7) were captured after 24-hour incubation with the MIONPs. It was observed that the control HeLa cells showed well-spread morphology with small microvilli on their surface (Fig. 6(a)). As the concentration of MIONPs increased from 0.05 mg/ml (inset of Fig. 6(b)) to 0.40 mg/ml (inset of Fig. 6(c)), the nanoparticles were observed to be bound on the cell surfaces. There were more bound nanoparticles at higher MIONP concentration as we can observe more nanoparticles bound

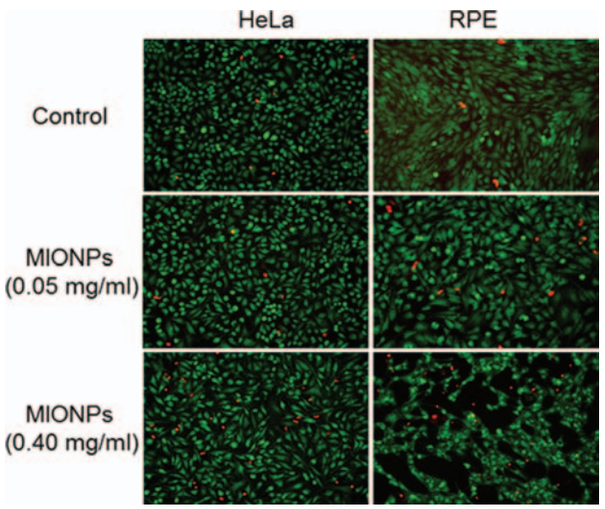

Fig. 4. Fluorescence images of HeLa cells and RPE cells treated with no MIONPs (control), 0.05 mg/ml MIONPs and 0.40 mg/ml MIONPs are shown in the left and right panels, respectively. Green fluorescence signals indicate living cells and red fluorescence signals indicate dead cells. (Objective magnification: ×10).

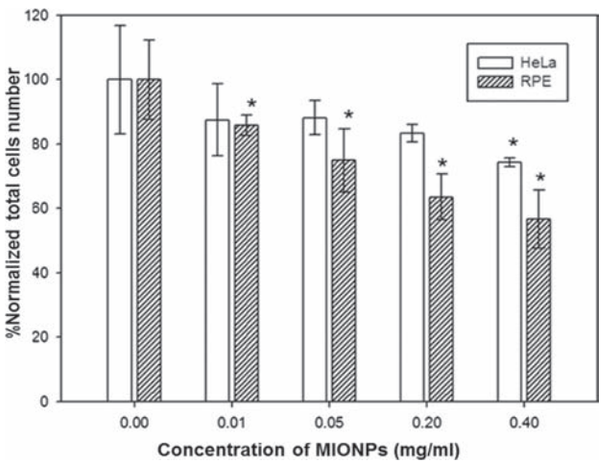

Fig. 5. Determination of relative cell numbers after 24-hour treatment with different concentrations of the MIONPs (0–0.40 mg/ml). ($n = 5$, $^{*}p < 0.05$ compared to control group of each cell line).

to the cells in Figure 6(c) than Figure 6(b). Microvilli are a typical morphological feature of HeLa cells,[34] the MIONPs were found to stimulate the appearance and the growth of microvilli on the cell surface (insets in Figs. 6(b) and (c)). Similar phenomenon was also observed by Ho and his co-workers.[35] For the HeLa cells after treatment with 0.40 mg/ml MIONPs, the cell number reduced significantly in the live/dead assay result (Fig. 5). Under SEM observation, this cell number reduction of HeLa cells can be observed along with the aberrations of cell morphology (Fig. 6(c)). At higher magnification, it can be seen more clearly that abundant microvilli projected from the cell surface and intertwined with the MIONPs (Figs. 6(d)–(f)). On the other hand, the MIONPs at lower concentrations were found to be not acutely toxic to the HeLa cells in the live/dead assay result (Fig. 5); however, they exhibited significant influence on the cell behavior and stimulated the appearance and growth of microvilli on the cell surface (Fig. 6(b)). The observation of microvilli stimulated at low concentrations of MIONPS indicates that the cell morphological changes can take place even though no toxic effect of these MIONPs at low concentrations was reflected in the traditional cell viability assay.

Under SEM observation, the control RPE cells were flat and well-spread in Figure 7(a). In the treatment groups, there were fewer microvilli on the RPE cell surfaces compared to the HeLa cells, and no obvious intertwining of microvilli with the MIONPs on the RPE cells was observed. Instead, there were some "bumps" stimulated on the RPE cell membranes after their incubation with the MIONPs as shown in Figure 7(b). The MIONPs at high concentration (0.40 mg/ml) caused large aberrations of the cell morphology (Fig. 7(c)). On closer inspection, the bumps on the RPE cell surface can be observed clearly as indicated by the red arrows in Figures 7(d)–(f). It is reported that the bumpy cell morphology is an indication of nanoparticle uptake.[12, 36] Thus, the bumps appearing on

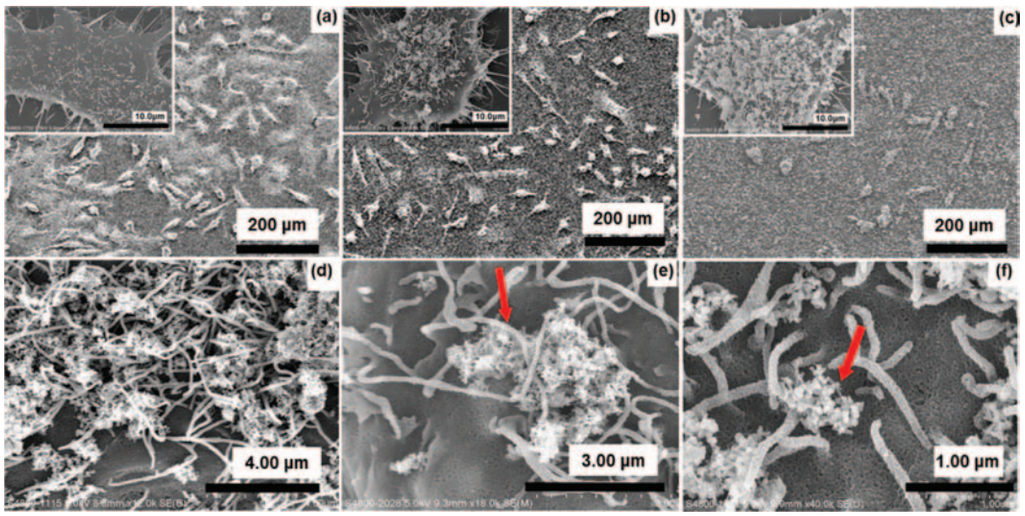

Fig. 6. SEM images of the HeLa cells after 24-hour exposure to MIONPs. Cell morphology of HeLa cells incubated with (a) no MIONPs, (b) 0.05 mg/ml MIONPs, and (c) 0.40 mg/ml MIONPs. Insets in (a), (b), and (c) are high magnification images of single HeLa cell in each group, scale bar = 10.0 μm. The MIONPs and microvilli on the HeLa cells incubated with 0.40 mg/ml MIONPs were imaged with different magnifications of (d) × 12 k, (e) ×18 k, and (f) ×40 k. In Figures 5(e) and (f), the red arrows indicated the MIONPs intertwined with the microvilli and attached on the cell surface.

the RPE cell surfaces evidence the internalization of the MIONPs which possibly led to the cell death.

The uptake of MIONPs into HeLa cells and RPE cells can be visualized in TEM images and confirmed by EDX measurements as shown in Figures 8 and 9. The EDX analysis indicates that the "black dots" in the TEM images contain the element of iron. The EDX results of the HeLa cell (Figs. 8(b1)–(b3)) and the RPE cell (Figs. 9(b1) and (b2)) are consistent with the presence of MIONPs that we could observe at different sites of the HeLa cell (Fig. 8(b)) and RPE cell (Fig. 9(b)) on the TEM images. Thus, the EDX analysis demonstrated the "black dots" are indeed iron oxide particles, and confirmed the uptake of MIONPs into HeLa cells and RPE cells.

However, the mechanism for the entry of MIONPs was different for the HeLa cells and the RPE cells. The red arrow in Figure 8(a1) and the site 2 circled in Figure 8(b) show the attachment of MIONPs on the cell surface and the

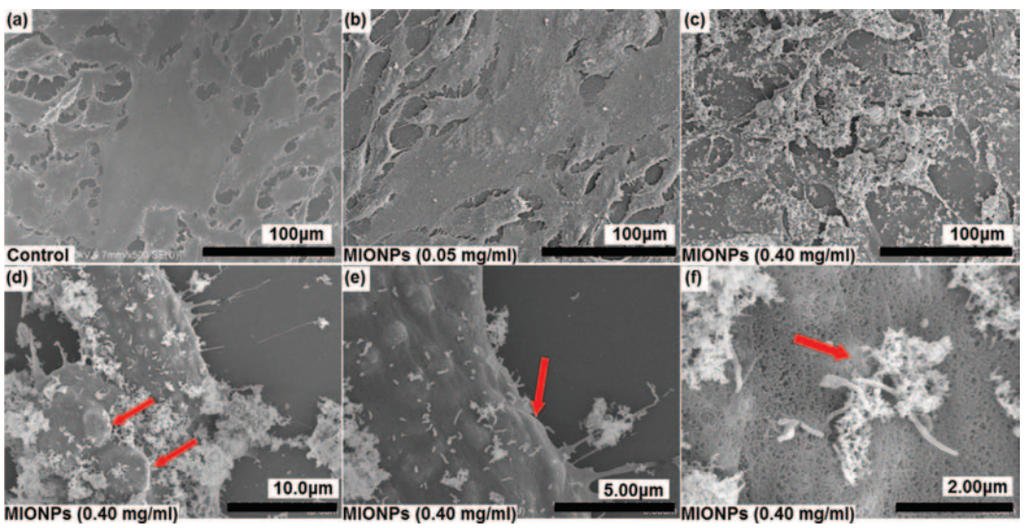

Fig. 7. SEM images of the RPE cells after 24-hour exposure to the MIONPs. Cell morphology of RPE cells incubated with (a) no MIONPs, (b) 0.05 mg/ml MIONPs, and (c) 0.40 mg/ml MIONPs. In Figure 6(a), the RPE cells incubated with no MIONPs are flat and well spread. In Figure 6(b), there are some bumps appearing on the RPE cell membrane when incubated with the MIONPs at a low concentration (0.05 mg/ml). In Figure 6(c), large aberrations of the cell morphology were caused when the RPE cells incubated with the MIONPs at a high concentration (0.40 mg/ml). The bumps on the RPE cells incubated with 0.40 mg/ml MIONPs were imaged with different magnifications of (d) ×4 k, (e) ×9 k, and (f) ×22 k. The red arrows in Figures 6(d)–(f) indicate the bumps on the RPE cells and the MIONPs attached on the cell surface.

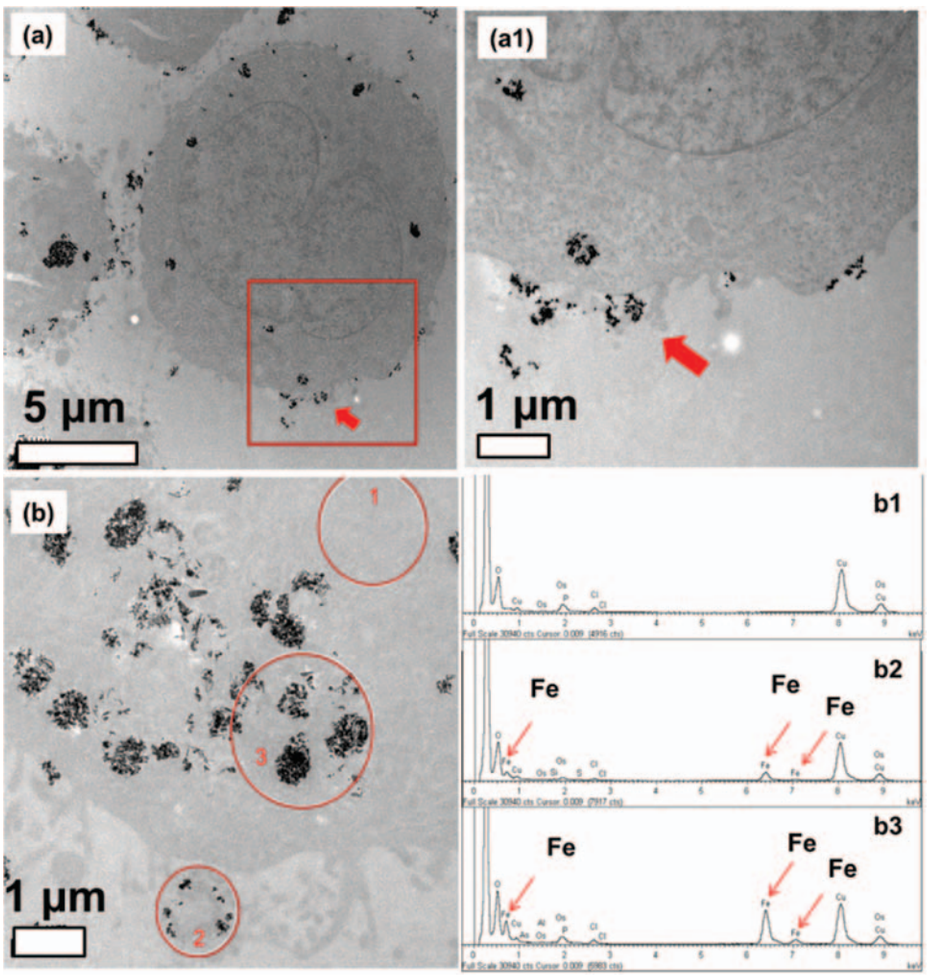

Fig. 8. TEM images and EDX results of the HeLa cells after 24-hour exposure to the MIONPs. (a) Low magnification image of single HeLa cell. (a1) Enlarged TEM image of the selected area in (a). The red arrow indicates the intertwining between the MIONPs and the microvilli on HeLa cell surface. (b) High magnification image of local area in HeLa cell. Site 1 includes only cell tissue, site 2 includes cell microvilli and MIONPs, and site 3 includes cell tissue and MIONPs. The (b1)–(b3) show the EDX results of site 1, site 2, and site 3 circled in (b) respectively, which confirm the presence of MIONPs.

RESEARCH ARTICLE

intertwining between the cell microvilli and the MIONPs, which are consistent with the phenomena observed in the SEM images (Figs. 6(e) and (f)). It can be observed that some MIONPs were internalized into the HeLa cytoplasm forming the vacuoles (site 3 in Fig. 8(b)). On the basis of these observations, the entry of the MIONPs into the HeLa cells can be attributed to endocytosis through the microvilli.[37] In contrast, there were fewer microvilli and no obvious intertwining of microvilli with MIONPs was found on the RPE cell surface. Therefore, it is unlikely that the MIONPs enter the RPE cells through the microvilli. As observed in Figure 9(a), the majority of MIONPs were engulfed by the RPE cells, which indicates the entry of MIONPs into the RPE cells was through phagocytosis. In phagocytosis, phagocyte pseudopods move circumferentially around the MIONPs until fusing at their distal tips, and then the process is accompanied by the formation of bumps on the RPE cell surfaces.[38, 39] The formation of bumps can indeed be observed in the SEM images (indicated by the red arrow in Figs. 7(d) and (e)) on the RPE cells. The different mechanisms for the uptake of MIONPs into HeLa cells and RPE cells should be one of the important reasons why the RPE cells were more susceptible to the MIONPs than the HeLa cells as shown in the live/dead assay results. Previously, it was reported that the uptake of MIONPs can result in cell morphological changes,[14] disruption of the cell membrane, disorganized cell cytoskeleton,[11, 15] and eventual cell death.[12] As such, different uptake mechanism of MIONPs can result in different cellular response because of different amount of MIONPs uptake. As shown in Figure 8, the MIONPs internalized into the HeLa cells through microvilli via endocytosis were smaller in size and less in amount than the ones engulfed into the RPE cells. This can be the reason for the HeLa cells showing higher tolerance with the MIONPs. In contrast, the RPE cells could uptake more and

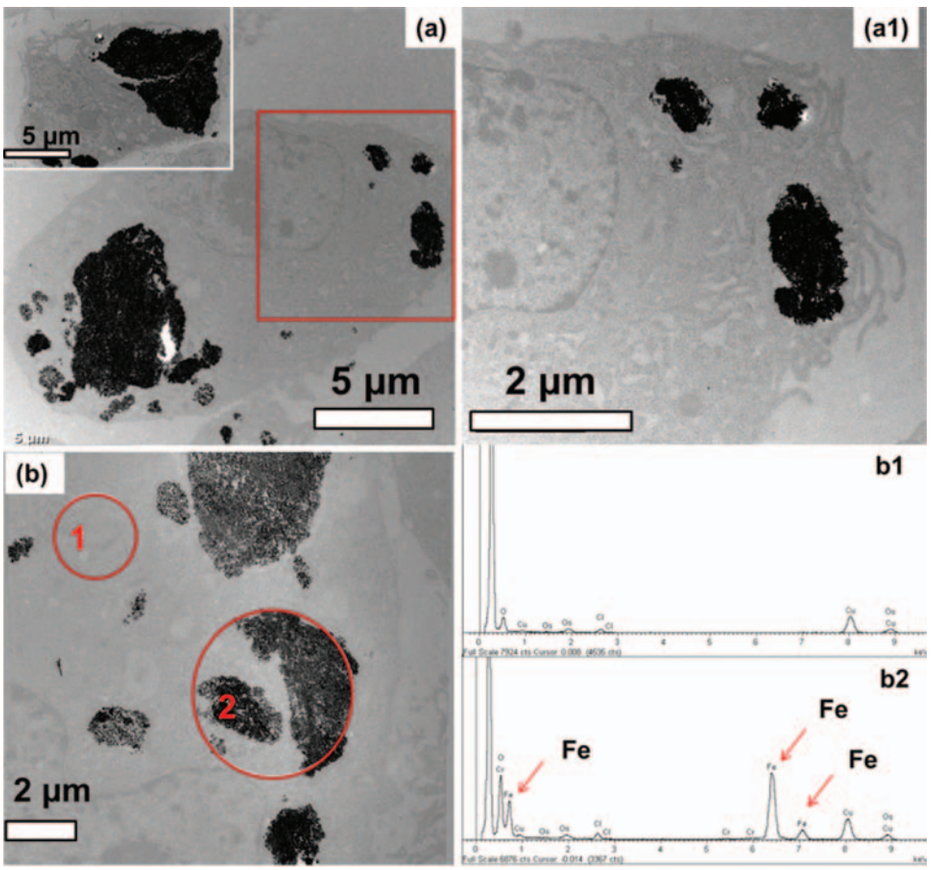

Fig. 9. TEM images and EDX results of the RPE cells after 24-hour exposure to the MIONPs. (a) Low magnification image of a single RPE cell. The inset shows the RPE cell suffering from particles overload. (a1) Enlarged TEM image of the selected area in (a). (b) High magnification image of local area in RPE cell. Site 1 includes only cell tissue, and site 2 includes cell tissue and MIONPs. The (b1) and (b2) show the EDX results of site 1 and site 2 circled in (b) respectively, which confirm the presence of MIONPs.

bigger MIONPs through phagocytosis, and thus the RPE cells were at higher risk of toxic effects from particle overload. The inset in Figure 9(a) shows the RPE cell suffered from the internalized particles occupying near half of its cell body. Thus, the cytotoxicity of the MIONPs showed cell-type dependence, because of the different mechanism for the entry of MIONPs into the HeLa cells and the RPE cells.

4. CONCLUSION

In this work, the uncoated MIONPs at a high concentration (0.40 mg/ml) were toxic to both HeLa cells and RPE cells while low concentrations of the MIONPs showed cell-type specific cytotoxicity. The MIONPs at low concentrations did not exhibit acute cytotoxicity on the HeLa cell viability in live/dead assay. However, strong intertwining between the nanoparticles and the microvilli was found on the HeLa cell surfaces under SEM, and some MIONPs entered into the HeLa cell cytoplasm as demonstrated by TEM observation and EDX analysis. This implies the cell morphological changes and the uptake of nanoparticles can take place even though no toxic effect of these MIONPs at low concentrations was reflected in the traditional cell viability assay. We also found that the normal human cell line (RPE cells) was more susceptible to the MIONPs than the cancer cell line (HeLa cells), and the MIONPs resulted in a dose-dependent cytotoxicity on the RPE cells. The effects of the MIONPs on cellular morphology and the cellular uptake of nanoparticles were different on these two cell lines. In comparison with the HeLa cells, there were fewer microvilli on the RPE cell surfaces and no obvious intertwining of microvilli with the MIONPs on the RPE cells was observed. Instead, there were bumps appearing on the RPE cell membranes and many more MIONPs internalized by RPE cells through the process of phagocytosis. Thus, the cytotoxicity of uncoated MIONPs shows cell-type dependence and it should be studied carefully on different cell types. In particular, the bioapplications of MIONPs on normal human cells should be undertaken with well-controlled concentrations since their cytotoxicity varies with their concentration.

Acknowledgments: This work was supported by the Seed Funding for Basic Research of the University of

Hong Kong and the General Research Fund of the Research Grants Council (HKU 704911P). Assistance from Dr. W. Y. Lui, Dr. Alice S. T. Wong, Dr. April M. Chow, Dr. T. H. Zheng and Mr. Z. Q. Lei at the University of Hong Kong, Ms. X. Chen and Ms. Y. Zhou at Hong Kong Baptist University is also gratefully acknowledged.

References and Notes

1. H. Kojima, Y. Mukai, K. Kamei, M. Morita, T. Inubushi, T. Yamamoto, Y. Yoshioka, N. Okada, S. Seino, and S. Nakagawa, *Ejc. Suppl.* 7, 172 **(2009)**.
2. K. Briley-Saebo, S. A. Hustvedt, A. Haldorsen, and A. Bjornerud, *J. Magn. Reson. Imaging* 20, 622 **(2004)**.
3. E. Wu, H. Tang, and J. Jensen, *Nmr. Biomed.* 17, 478 **(2004)**.
4. C. Lu, Y. Hung, J. Hsiao, M. Yao, T. Chung, Y. Lin, S. Wu, S. Hsu, H. Liu, and C. Mou, *Nano Lett.* 7, 149 **(2007)**.
5. M. Lewin, N. Carlesso, C. Tung, X. Tang, D. Cory, D. Scadden, and R. Weissleder, *Nat. Biotechnol.* 18, 410 **(2000)**.
6. C. Plank, F. Scherer, U. Schillinger, C. Bergemann, and M. Anton, *Journal of Liposome Research* 13, 29 **(2003)**.
7. J. Dobson, *Drug Dev. Res.* 67, 55 **(2006)**.
8. C. Sun, J. Lee, and M. Zhang, *Advanced Drug Delivery Reviews* 60, 1252 **(2008)**.
9. A. Jordan, R. Scholz, P. Wust, and H. Fahling, *J. Magn. Magn. Mater.* 201, 413 **(1999)**.
10. A. Ito, M. Shinkai, H. Honda, and T. Kobayashi, *Cancer Gene Therapy* 8, 649 **(2001)**.
11. A. Gupta and M. Gupta, *Biomaterials* 26, 1565 **(2005)**.
12. C. Berry, S. Wells, S. Charles, and A. Curtis, *Biomaterials* 24, 4551 **(2003)**.
13. C. Berry, S. Wells, S. Charles, G. Aitchison, and A. Curtis, *Biomaterials* 25, 5405 **(2004)**.
14. A. Gupta and A. Curtis, *Biomaterials* 25, 3029 **(2004)**.
15. A. Gupta and A. Curtis, *Journal of Materials Science: Materials in Medicine* 15, 493 **(2004)**.
16. M. Mahmoudi, A. Simchi, H. Vali, M. Imani, M. Shokrgozar, K. Azadmanesh, and F. Azari, *Adv. Eng. Mater.* 11, B243 **(2009)**.
17. M. Mahmoudi, A. Simchi, A. S. Milani, and P. Stroeve, *J. Colloid Interface Sci.* 336, 510 **(2009)**.
18. M. Mahmoudi, A. Simchi, and M. Imani, **(2009)**.
19. M. Mahmoudi, A. Simchi, M. Imani, M. Shokrgozar, A. Milani, U. Hafeli, and P. Stroeve, *Colloids and Surfaces B: Biointerfaces* **(2009)**.
20. U. O. Häfeli, J. S. Riffle, L. Harris-Shekhawat, A. Carmichael-Baranauskas, F. Mark, J. P. Dailey, and D. Bardenstein, *Molecular Pharmaceutics* 6, 1417 **(2009)**.
21. T. Pisanic, J. Blackwell, V. Shubayev, R. Finones, and S. Jin, *Biomaterials* 28, 2572 **(2007)**.
22. S. Laurent, D. Forge, M. Port, A. Roch, C. Robic, L. Vander Elst, and R. Muller, *Chem. Rev.* 108, 2064 **(2008)**.
23. L. Wang, D. Nagesha, S. Selvarasah, M. Dokmeci, and R. Carrier, *Journal of Nanobiotechnology* 6, 11 **(2008)**.
24. A. Jordan, P. Wust, R. Scholz, B. Tesche, H. Fahling, T. Mitrovics, T. Vogl, J. Cervos-Navarro, and R. Felix, *International Journal of Hyperthermia* 12, 705 **(1996)**.
25. M. Maurer-Jones, K. Bantz, S. Love, B. Marquis, and C. Haynes, *Nanomedicine* 4, 219 **(2009)**.
26. N. Lewinski, V. Colvin, and R. Drezek, *Small* 4, 26 **(2008)**.
27. A. Tomitaka, A. Hirukawa, T. Yamada, S. Morishita, and Y. Takemura, *J. Magn. Magn. Mater.* 321, 1482 **(2009)**.
28. A. Petri-Fink, B. Steitz, A. Finka, J. Salaklang, and H. Hofmann, *European Journal of Pharmaceutics and Biopharmaceutics* 68, 129 **(2008)**.
29. T. Xia, M. Kovochich, M. Liong, J. I. Zink, and A. E. Nel, *ACS Nano* 2, 85 **(2007)**.
30. N. Kohler, C. Sun, J. Wang, and M. Zhang, *Langmuir* 21, 8858 **(2005)**.
31. J. Christie and U. Kompella, *Drug Discovery Today* 13, 124 **(2008)**.
32. T. W. Prow, *Wiley Interdisciplinary Reviews: Nanomedicine and Nanobiotechnology* 2, 317 **(2010)**.
33. S. Hussain, K. Hess, J. Gearhart, K. Geiss, and J. Schlager, *Toxicology In Vitro* 19, 975 **(2005)**.
34. L. Jiang, Y. Sun, and X. Chen, *Small, n/a* **(2011)**.
35. V. Ho, A. Barcza, R. Chen, K. Muller, N. Darton, and N. Slater, *Biomaterials* 30, 6548 **(2009)**.
36. L. Williams, H. Lew, B. Shannon, C. Singley, F. Davidorf, R. Jin, and J. Wolinsky, *The American Journal of Pathology* 142, 451 **(1993)**.
37. E. Illés and E. Tombácz, *J. Colloid Interface Sci.* 295, 115 **(2006)**.
38. A. J. Gomes, C. N. Lunardi, F. H. Caetano, L. O. Lunardi, and A. E. H. Machado, *Microsc. Microanal.* 12, 399 **(2006)**.
39. J. Aggeler and Z. Werb, *The Journal of Cell Biology* 613 **(1982)**.

Received: 1 January 2012. Accepted: 15 June 2012.

RESEARCH ARTICLE